Nuclear quadrupole interaction at ^{44}Sc in the anatase and rutile modifications of TiO_2: Time-differential perturbed-angular-correlation measurements and *ab initio* calculations

Seung-baek Ryu, Satyendra K. Das,* and Tilman Butz†
Universität Leipzig, Fakultät für Physik und Geowissenschaften, Institut für Experimentelle Physik II, Linnéstrasse 5, 04103 Leipzig, Germany

Werner Schmitz
Universität Leipzig, Fakultät für Chemie und Mineralogie, Institut für Mineralogie, Kristallographie und Materialwissenschaft, Scharnhorststrasse 20, 04275 Leipzig, Germany

Christian Spiel, Peter Blaha, and Karlheinz Schwarz
Technische Universität Wien, Institut für Materialchemie, Getreidemarkt 9, 1060 Vienna, Austria
(Received 27 November 2007; revised manuscript received 31 January 2008; published 21 March 2008)

The nuclear quadrupole interaction of the first excited $I=1$ state of ^{44}Sc in the anatase and rutile modifications of bulk TiO_2 was determined by time-differential perturbed-angular correlation of γ rays. New $LaBr_3$(Ce) scintillators with excellent energy resolution allowed us to separate the 68 and 78 keV lines of the γ-γ cascade. For anatase, an almost axially symmetric electric field gradient (EFG) with an asymmetry parameter of $\eta=0.10(1)$ and a nuclear quadrupole frequency of $\omega_Q=9.29(3)$ Mrad/s was obtained. For rutile, an almost antiaxial EFG with $\eta=0.94(1)$ and $\omega_Q=16.14(6)$ Mrad/s was obtained, which contradicts literature values. *Ab initio* calculations of the EFG using the WIEN2K code were performed for anatase and rutile for pure systems as well as for relevant impurities, such as Sc and Cd on Ti sites. The nuclear quadrupole moment of the $I=1$ state in ^{44}Sc is redetermined with a sevenfold improved accuracy to be $Q=\pm 0.214(3)$ b.

DOI: 10.1103/PhysRevB.77.094124 PACS number(s): 61.66.Fn, 76.80.+y, 71.15.Ap, 61.05.cp

I. INTRODUCTION

Bulk TiO_2 is widely used as a white pigment in paints, lipsticks, toothpaste, drugs, and chewing gum, to name just a few. Its prominent modifications are anatase and rutile. The latter is the high-temperature modification, which is retained upon cooling. The structure of anatase is tetragonal, with space group $I4_1/amd$ (141) and with two alternative cell settings.

Anatase (1): Ti^{4+}: 0, 0, 0; O^{2-}: 0, 0, z [$z=0.208\ 06(5)$].[1]

Anatase (2): Ti^{4+}: 0, 1/4, 3/8; O^{2-}: 0, 1/4, z [$z=0.166\ 86(5)$].[2]

The structure of rutile is also tetragonal, with space group $P4_2/mnm$ (136) and without alternative setting.

Rutile: Ti^{4+}: 0, 0, 0; O^{2-}: u, u, 0 [$u=0.30477(6)$].[1,2]

The point symmetry of Ti is $\bar{4}m2$ in anatase and $2/m\ 2/m\ 2/m$ in rutile; therefore, in anatase, the electric field gradient (EFG) should be axially symmetric by symmetry. For oxygen, it is $2mm$ in both TiO_2 modifications. Both polymorphs are insulators with band gaps of 3.06 eV (rutile) and 3.20 eV (anatase).[3] The possibility to produce nanoparticles of TiO_2, which are transparent for the visible light and absorb UV, led to the use of such particles as physical filters in sunscreens without the whitening effect. Due to their good crystallinity, they are photocatalytically active and, hence, used for wastewater purification.[4] From a nuclear physics point of view, TiO_2 (rutile) has been used as a matrix for the implantation of foreign atoms for the determination of nuclear quadrupole moments using Fourier transform nuclear magnetic resonance (FT-NMR).[5]

This paper presents the following: (i) conflicting results have been reported for the nuclear quadrupole interaction (NQI) of ^{44}Sc in rutile determined by time-differential perturbed-angular correlation[6] (TDPAC) and of ^{45}Sc in rutile determined by FT-NMR,[5] which requires clarification. (ii) The NQI for ^{47,49}Ti in anatase has been determined by NMR; however, the NQI for ^{44}Sc in anatase has not been determined. The calculation of the EFG tensor in both modifications of TiO_2 for the pure and impurity systems is rather challenging and reveals the strength and limitations of the *ab initio* calculations by using the WIEN2K code. (iii) The nuclear quadrupole moment for the first excited state in ^{44}Sc is known with an accuracy of about 10% only;[25] for future EFG studies, it is desirable to reduce this uncertainty. (iv) Since rather unexpected results for the EFG for various impurities on Ti sites[7] in rutile compared to Ti atoms themselves[8] were reported, which include unusual temperature dependencies, a clarification is required.

II. EXPERIMENT

Bulk TiO_2 was prepared as follows: Ti-tetra-isopropoxide was added dropwise in 6*M* HCl solution with constant stirring. A white precipitate was formed but dissolved when stirred. After the whole precipitate was dissolved, concentrated ammonium hydroxide was added dropwise to this liquid. A white precipitate formed in this process, and was filtered and thoroughly washed with water to remove the ammonium chloride formed in the solution. The precipitate was then heated at different temperatures to obtain TiO_2 of different modifications. To obtain radio-labeled TiO_2 with ^{44}Ti, a tracer in HCl medium was added to the initial 6*M* HCl solution before the addition of Ti-tetra-isopropoxide. An excess ammonia solution was added to ensure the complete

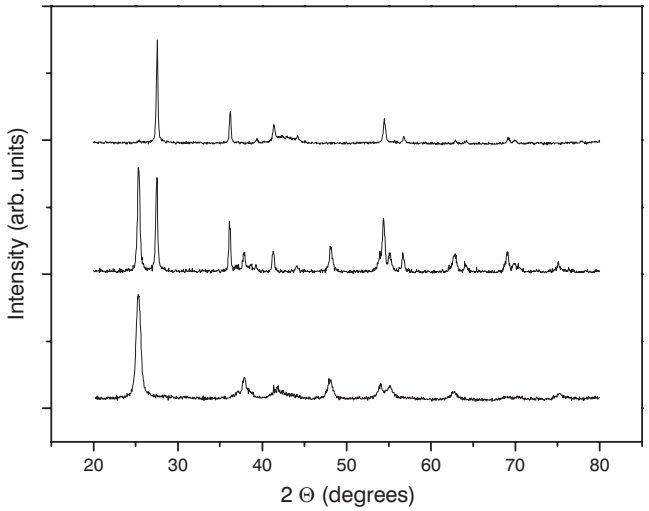

FIG. 1. From top to bottom: x-ray diffractograms for pure rutile, a mixture of rutile and anatase, and pure anatase. The top and bottom data were obtained from the same radio-labeled samples, which were used for the TDPAC measurements, whereas the middle one was taken from an inactive sample separately prepared.

precipitation of Ti. After drying, the powder was heated in air to obtain bulk TiO_2. This sample was annealed at 823 K for 0.5 h and it was found to have the anatase structure, which was confirmed by x-ray diffraction (XRD). XRD of small amounts of the labeled material was carried out using the Bragg–Brentano geometry. Both the XRD peaks (see Fig. 1, bottom) and the NQI frequency (see Fig. 2, bottom) exhibited some broadening, which indicates imperfect crystallinity.

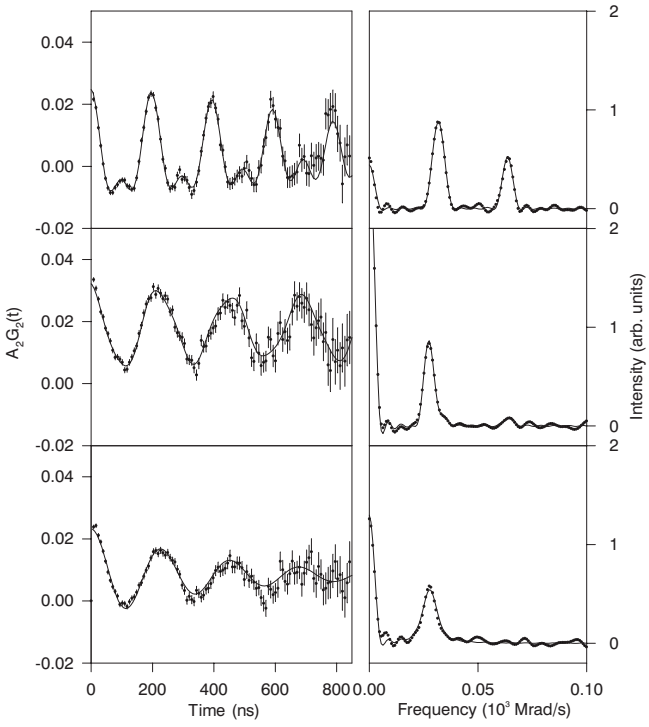

FIG. 2. From top to bottom: (left) TDPAC spectra taken at 300 K for ^{44}Sc in pure rutile, anatase with a small admixture of rutile, and pure anatase and (right) the corresponding cosine transforms of the TDPAC spectra.

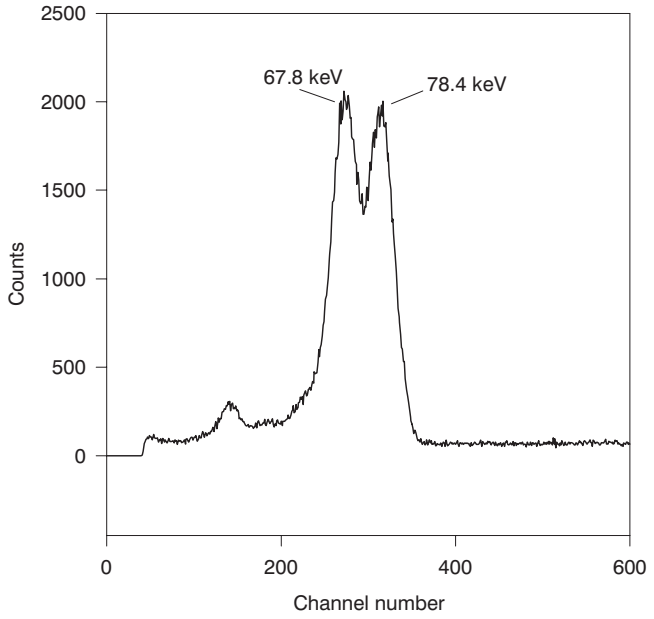

FIG. 3. γ-ray spectrum of ^{44}Ti using $LaBr_3$(Ce) scintillators. The 67.8 and 78.4 keV lines are sufficiently well separated.

Heating the dried precipitate further up to 1098 K for 0.5 h led to a considerable line narrowing and hence to a good crystallinity; however, as will be shown below, part of the material was already converted to rutile (see Fig. 1, middle and Fig. 2, middle). Heating the sample to 1123 K for 2 h finally yielded the rutile modification (see Fig. 1, top and Fig. 2, top). In each case, the sample was allowed to slowly cool to room temperature. The time was 4–5 h depending on the annealing temperature.

TDPAC measurements of the 78–68 keV γ-γ cascade at room temperature were carried out using a TDPAC camera,[9] which consists of six $LaBr_3$(Ce) scintillators (12 mm diameter and 12 mm height) mounted on XP2020URQ photomultipliers. These new scintillators have excellent energy resolution and good timing properties. Both the 68 and 78 keV lines could just be resolved (see Fig. 3). We selected the lower half of the 68 keV peak and the upper half of the 78 keV peak and could thus obtain TDPAC spectra, which decayed to one side only without leakage to the other side, as was always the case thus far. The advantage is that the signal to the uncorrelated background is improved by a factor of 2 compared to earlier studies, which is particularly needed for low frequencies, as is the case in the present study. The time resolution was 750 ps (full width at half maximum) for these energy settings. This is more than sufficient for the present purpose because the observed frequencies are rather low. The long half-life of the intermediate state of about 150 ns makes the detection of delayed coincidences up to about 800 ns feasible.

The NQI of the $I=1$ intermediate state leads to a splitting with eigenvalues of $E_{1,2}=1\pm\eta$ and $E_3=-2$ in units of $\omega_Q=eQV_{zz}/4\hbar$. Here, Q denotes the nuclear quadrupole moment

of the $I=1$ state and V_{zz} is the largest component in magnitude of the EFG tensor. Hence, the observed quadrupole frequencies in a TDPAC spectrum are $\omega_1=2\eta\omega_Q$, $\omega_2=(3-\eta)\omega_Q$, and $\omega_3=(3+\eta)\omega_Q$. The perturbation function then reads[10]

$$G_{22}(t)=\frac{2}{5}+\frac{1}{5}\cos\,\omega_1 t+\frac{1}{5}\cos\,\omega_2 t+\frac{1}{5}\cos\,\omega_3 t.$$

This means that for $\eta=0$, we have one frequency only and an elevated hard core; i.e., the time-independent contribution of the perturbation function is 3/5. For $\eta=1$, on the other hand, we have two frequencies: ω_1 and ω_2 coincide and ω_3 is just twice as large. In order to account for a finite distribution in ω_Q, which is assumed to be Lorentzian, each of the cosine terms—but not the hard core—is multiplied by the factor $\exp(-\delta\omega_n t)$, where δ denotes the half-width at half maximum of the distribution function.

III. THEORY

Theoretical calculations based on the density functional theory (DFT) have been performed with the augmented plane wave plus local orbital (APW+LO) method, as embodied in the WIEN2K code.[11] We used the recently proposed generalized gradient approximation (GGA) of Wu and Cohen (WC-GGA),[12] which yields, on average, better results for solids[13] than the standard GGA.[14] Well converged basis sets (RKMAX=7) include extra local orbitals for the semicore states (metal has 3*s* and 3*p* and oxygen has 2*s*). In order to ensure proper variational freedom of the basis set for a sensitive quantity such as the EFG, we also added additional local orbitals for the metal 3*d* (expanded at the energies of O 2*s*) and the O 2*p* states (expanded at the metal 3*p* energies). We used the experimental lattice parameters but optimized the internal position parameters of all atoms. It has been shown before[15] that even small changes in the positions can have large effects on the EFG and even more on the asymmetry parameter η. The impurity calculations have been done using $2\times2\times3$ (rutile, 72 atoms) and $2\times2\times1$ (anatase, 48 atoms) supercells with full relaxation of all atomic positions. Since these supercell calculations (must) lead to metallic solutions, we have also added one (Sc) or two (Cd) electrons (compensated by a constant background charge) in order to establish an insulating system. The EFGs were obtained from the self-consistent potentials without further approximations.[16]

IV. EXPERIMENTAL RESULTS

The TDPAC spectrum for anatase, which is prepared at 823 K, is shown in Fig. 2 (bottom) together with its cosine transform. At first glance, it seems that an axially symmetric EFG prevails and that there is a small damping due to a small distribution of EFGs, which are assumed to be Lorentzian. However, a careful inspection of the linewidth of the zero-frequency peak shows that this peak is slightly broader than the experimental resolution. The $m=\pm1$ degeneracy is lifted for a deviation from the axial symmetry, and a rather low frequency component evolves from $\omega=0$ for small η.

TABLE I. TDPAC parameters for the anatase (ana) and rutile (rut) modifications of TiO_2.

Parameters	Anatase	Mixed	Rutile
A_{22} (effective)	0.033(1)	0.036(2)	0.035(1)
$\omega_Q^{(ana)}$ (Mrad/s)	9.29(3)	9.29	
$\eta^{(ana)}$	0.10(1)	0	
$\delta^{(ana)}$	0.084(8)	0	
$\omega_Q^{(rut)}$ (Mrad/s)		16.14	16.14(6)
$\eta^{(rut)}$		0.94	0.94(1)
$\delta^{(rut)}$		0.028(15)	0.003(5)
Fraction (%)	100	76+24	100

Hence, we analyzed the data, which allow for a small η in addition to a small line broadening. Clearly, this conventional way to analyze the data is just a crude approximation to the actual situation. However, for $I=1$, there is no chance to derive parameters, which unambiguously describe the two-dimensional distribution function. In view of the relatively small distribution width δ, this approximation is well justified. Further heating the sample to 873 K resulted in a slightly reduced line broadening but left all other parameters unchanged. The least-squares fitting analysis yielded $\omega_Q=9.29(3)$ Mrad/s and $\eta=0.10(1)$.

Heating the dried powder to 1098 K for 30 min led to a mixture of anatase and rutile (see Fig. 2, middle). When analyzing the spectrum with the hyperfine parameters for pure anatase and pure rutile (see below), we obtain an admixture of rutile of 24(3)%. It should be mentioned that the XRD data shown in Fig. 1 (middle) were taken on a sample without ^{44}Ti labels, which was prepared in exactly the same way as the labeled one; however, the percentage of the admixture of rutile was much larger. Evidently, minute differences in sample preparation modify the transition temperatures, which is not surprising considering the wide range of transition temperatures reported in the literature. Further heating to 1123 K for 2 h led to the complete conversion to rutile. As shown in Fig. 2 (top), the TDPAC spectrum clearly shows a fundamental frequency and its harmonic, as is characteristic for η close to 1. The least-squares fitting analysis yielded $\omega_Q=16.14(6)$ Mrad/s and $\eta=0.94(1)$. All fitted hyperfine parameters are listed in Table I.

V. THEORETICAL RESULTS

As mentioned above, the EFG is very sensitive to very small changes in the atomic positions. Even for the pure materials (anatase and rutile), where accurate structural parameters are available, the spread of the experimental position is large enough to change the calculated EFG values, and for the impurity cases, no experimental information about possible relaxations is available. On the other hand, the EFG is rather insensitive to small changes in lattice parameters, and the experimental data are much more accurate than theoretically calculated lattice parameters, which usually have an error of about 1%. Thus, we have used the experi-

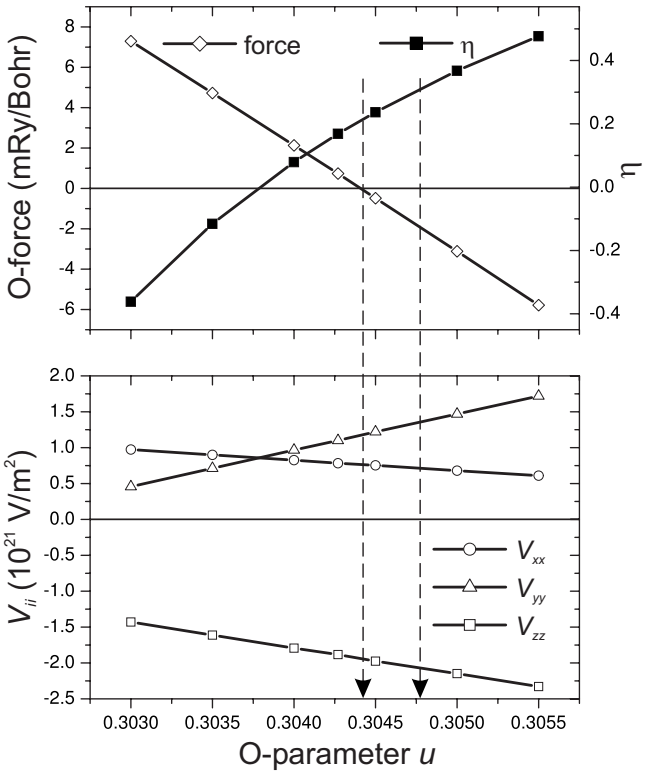

FIG. 4. Dependence of the theoretical Ti EFG tensor V_{ii} in rutile (lower panel) as a function of the internal O parameter u. In the upper panel, the corresponding asymmetry parameter and the theoretical force on the O atom is also shown. The vertical arrows indicate theoretical (left) and experimental (right) u parameters.

mental lattice parameters, but optimized the free internal atomic parameters.

For anatase and rutile, we obtain the oxygen parameters $z=0.166\ 12$ (second settings) and $u=0.304\ 42$ (see Fig. 4), which can be compared to, e.g., $z=0.166\ 86$ (Ref. 2) or $z=0.166\ 94$ (Ref. 1) and $u=0.304\ 77$ (Refs. 1 and 2), respectively. For the impurity cases, we list the results of the nearest neighbor relaxations in Table II. One can see that the Ti-O distances for anatase and rutile agree with the experiment to within a few thousandths of an angstrom, while for the impurities, strong relaxations are found.

The Sc/Cd-O distances are up to 10% larger than Ti-O distances and the d_1/d_2 ratio (see Table II for definition) is not constant, but d_1 becomes even larger than d_2. As already explained by Errico *et al.*,[17] this happens because an increase in d_2 leads to an equal decrease in the neighboring Ti-O distances, while an increase in d_1 only slightly decreases the neighboring Ti-O distances. The differences in relaxation for neutral or charged impurities are rather small. The relaxations around the Cd impurity in rutile are in reasonable agreement with those in Ref. 17 [which used local density approximation (LDA) instead of WC-GGA employed in the present calculations], but significantly deviate from those in Ref. 18.

The results of the WIEN2K EFG calculations for Ti, Sc, and Cd in anatase and rutile are listed in Tables III and IV. It should be noted that the results for Cd in rutile depend strongly on whether or not electrons are added to Cd; while for Sc, this has a much smaller influence.

TABLE II. Theoretical and experimental metal-oxygen distances d (in Å) for various systems. d_1 and d_2 refer to distances between Me and four and two oxygen neighbors, respectively.

System	Theor./expt. Me-O d_1	Theor./expt. Me-O d_2
Anatase Ti	1.934/1.933 (Ref. 2)	1.982/1.987(Ref.2)
Anatase Sc	2.015	2.120
Anatase Sc+$1e^-$	2.012	2.111
Anatase Cd	2.099	2.184
Anatase Cd+$2e^{2-}$	2.088	2.320
Rutile Ti	1.950/1.949	1.978/1.980
Rutile Sc	2.068	2.055
Rutile Sc+$1e^-$	2.066	2.055
Rutile Cd	2.193	2.128
Rutile Cd+$2e^{2-}$	2.203	2.126

VI. DISCUSSION

A. Anatase

The theoretical and experimental EFGs for Ti in anatase are in reasonable agreement, but are certainly not perfect. Part of that could be due to finite temperature effects in the measured EFGs. On the other hand, using the experimental structural parameter with a slightly modified oxygen z parameter (by 0.00074) already modifies the theoretical EFG by 30%. It should be mentioned further that it is sometimes argued that the DFT calculations overestimate the O p-Ti d interactions and some enhanced treatment of the stronger correlated Ti d electrons is necessary. Using the LDA+U method (with $U=3.5$ eV) enhances the theoretical EFG again by 6%.

To our knowledge, the NQI at ^{44}Sc in anatase has not been determined before. Experimentally, we observe a unique site with almost axial symmetry. There are two Ti atoms in the unit cell; however, the two sites differ in orientation only and hence are not distinguishable in a powder sample. The crystal symmetry is $\bar{4}m2$ and thus η should be zero. We associate the very small η with the finite damping (line broadening), which appeared to be unavoidable because annealing the sample in order to reduce the linewidth is only possible at the disadvantage of initiating the conversion to rutile. Such a small deviation from axial symmetry has also been reported in Ref. 19. It is likely a consequence of the fact that powder spectra yield an average over nonzero η values at the individual nuclear sites rather than averages of EFG tensor components. In order to prove that the averages of V_{xx} and V_{yy} are, in fact, identical would require a single crystal work. The theoretical EFG for Sc in anatase is nearly twice as large as that in the experiment. Possible explanations could again be temperature effects or small errors in the large relaxations around Sc and also the limited size (48 atoms) of the supercell, which corresponds to a Sc concentration of

TABLE III. Experimental and theoretical results for EFGs in anatase.

System	T (K)	V_{zz} (10^{21} V/m^2)	η	Q (b)	Comments	Ref.
^{47,49}Ti in TiO_2	300	±0.761(7)	0.06(2)	+0.302/+0.247		19
Ti in TiO_2	0	+0.98	0		LAPW+LO	This work
^{44}Sc in TiO_2	300	±1.127(4)	0.10(1)	0.214(3)		This work
Sc in TiO_2	0	+2.06	0		LAPW+LO	This work
Cd in TiO_2	0	+1.37/+8.12 [a]	0		LAPW+LO	This work

[a]Second entry is for $+2e^-$.

6.25%. For a Cd impurity in anatase, we find a large influence of the charge added and the EFG changes by more than a factor of 6.

B. Rutile

Contrary to anatase, there are several experimental data and theoretical calculations of EFGs for pure rutile and for impurities in rutile. Table IV lists the available data for various metal sites. Similar to anatase, the calculated EFG in rutile crucially depends on the oxygen position (see Fig. 4). By using GGA instead of LDA[22] for the structural optimization, both the resulting V_{zz} and η are smaller compared to Ref. 22 and also somewhat smaller than room temperature experiments. The theoretical values imply $T=0$ and the extrapolation from 150 K, which is the lowest data point in Ref. 8, to 0 K yields $V_{zz}=1.95\times10^{21}$ V/m^2 and $\eta=0.25$. An earlier experiment[24] using dynamic nuclear polarization in rutile-TiO_2 doped with 0.2% Cr^{3+} gave slightly different values: $V_{zz}=2.30(10)/2.25(11)\times10^{21}$ V/m^2 for ^{47}Ti/^{49}Ti and $\eta=0.303(8)$. Because of the doping with Cr^{3+}, we shall not discuss it further here. For Sc in rutile, we observed a unique site and an almost antiaxial EFG, i.e., η near 1. The crystal symmetry is tetragonal, but the point group at Ti has a twofold rotational axis only and thus a nonzero η is possible. There are two Ti atoms in the unit cell; however, the two sites differ in orientation only and hence are not distinguishable in a powder sample.

There is good agreement for V_{zz} and η for both stable Ti isotopes in rutile using different techniques. The present cal-

TABLE IV. Experimental and theoretical results for EFGs in rutile.

System	T (K)	V_{zz} (10^{21} V/m^2)	η	Q (b)	Comments	Ref.
^{47,49}Ti	300	±2.14(10)[a]	0.19(1)	+0.302/+0.247	150–1500 K	8
^{49}Ti	300	±2.34	0.192(8)	+0.247	Single crystal	5
^{47,49}Ti	300	±2.33	0.20(2)	+0.302/+0.247		19
^{44}Sc	300	±2.02(19)	0.94(1)	0.214(3)		This work
^{45}Sc	300	±1.93(2)	0.983(3)	−0.236(2)	Single crystal	5
^{44}Sc	300	±1.93(20)	0	0.21(2)		6
^{93}Nb	300	±6.44(40)	0.463(7)	−0.32(2)	Single crystal	5
^{111}Cd	300	±5.75(2)[b]	0.18(1)	0.77	290–1300 K	7
^{111}Cd	300	±5.23(5)[b]	0.18(1)	0.83	290–1300 K	20
^{111}Cd	300	±5.34(1)[b]	0.18(1)	0.83	290–1300 K	21
^{181}Ta	300	±13.29(6)[b]	0.57(1)	2.51[c]	290–1300 K	7
Ti	0	−1.94	0.21		APW+LO	This work
Ti	0	−2.09	0.43		LAPW+LO, LDA	22
Ti	0	−2.66	0.67		Green's function	18
Sc	0	+2.05/+2.04[d]	0.67/0.75[d]		APW+LO	This work
Sc	0	−1.96	0.49		Green's function	18
Nb	0	−5.81	0.349		Green's function	18
Cd	0	+6.00/+5.00[d]	0.83/0.39[d]		APW+LO	This work
Cd	0	−7.16/+4.55[d]	0.91/0.26[d]		APW+LO, LDA	17
Cd	0	−5.09	0.39		Green's function	18
Ta	0	−11.76	0.34		Green's function	18

[a]Recalculated from Ref. 18; there is a factor of 10 discrepancy.
[b]Uncertainties in Q are apparently not included.
[c]Latest value of $Q=2.35(6)$ b (Ref. 23).
[d]Second entry for addition of $1e^-$ (Sc) or $2e^-$ (Cd).

culation is closest to the experimental data, especially as far as η is concerned. The Green's function technique greatly overestimates V_{zz} and η.[18]

The experimental values for V_{zz} and η for Sc in rutile derived by different techniques are in very good agreement, with the exception of the early work of Withnell and Glass.[6] Here, V_{zz} is in good agreement—maybe by chance—whereas the assumption of $\eta=0$ is certainly wrong. The authors remark that the interaction strength is nearly exactly the same as that found previously in $PbTiO_3$.[25] The time resolution should have been good enough to reveal the harmonic frequency, i.e., characteristic for $\eta=1$, which was not the case. We have no explanation for this discrepancy; however, excellent agreement between the present results and the FT-NMR result[5] renders the earlier result of Withnell and Glass[6] unlikely. The minute discrepancy in η between the present result $[\eta=0.94(1)]$ and the FT-NMR result[5] $[\eta=0.983(3)]$ could be due to the fact that in the latter case, 0.5% Sc was used, whereas in the present study, Sc is "infinitely" dilute. It is astonishing that η is close to unity, which is contrary to Ti in TiO_2. We believe that the lattice relaxation around the Sc impurity, as revealed by the metal oxygen distances listed in Table II and the extreme sensitivity of the EFG tensor components on the internal O parameter, are responsible for these differences. V_{zz} has even changed orientation compared to Ti and Nb in TiO_2,[5] which, however, is not unexpected in the vicinity of $\eta=1$. Again, agreement between experiment and theory is very good as far as V_{zz} is concerned, whereas the theoretical value for η is a bit too low, especially for the Green's function calculation.[18] It should be mentioned that although the magnitude of V_{zz} is quite similar between the present calculations and Ref. 18, the sign is different. This is also true for Cd in rutile, where previous calculations[17,18] find a negative sign for V_{zz}. However, in the latter case, η is close to 1 for the neutral system, thus the actual differences between Ref. 17 and the present calculations are small and probably due to the different exchange-correlation potential. The charge added impurity calculations lead to good agreement with experiment.

The agreement between experimental results for ^{93}Nb (Ref. 5) and ^{181}Ta in rutile and Green's function calculations[18] is good. Rather than to discuss these systems in more detail, we want to address another point, namely, the temperature dependence. Both for Ti and Cd on Ti sites in rutile-TiO_2, a small η was observed which goes to zero in approximately the middle of the investigated temperature range and then builds up again. This is in marked contrast to Ta on Ti sites in rutile-TiO_2, where a fairly large η was observed which is nearly temperature independent. This also suggests that for Sc on Ti sites in rutile-TiO_2, a very weak temperature dependence is expected.

The origin of this distinct temperature dependency in rutile probably lies in the extremely strong dependence of η on the internal O position u (see Fig. 4). When u is reduced by about 0.001, η decreases to zero and builds up again because V_{xx} and V_{yy} (both rotated by 45° with respect to the crystallographic axis) interchange their magnitude. Of course, the temperature dependence of η is due to a static change of u introduced not only by small thermal expansions but also by anisotropic thermal vibrations, which will enhance the effect. However, we cannot really explain in detail why Sc or Ta behave differently, except for speculating that small variations of u may not change the asymmetry parameter so much in these cases with large η. In conclusion, *ab initio* calculations of the electric field gradients in anatase and rutile are rather challenging and a detailed explanation of the differences between pure and impurity systems, which include their temperature dependences, has to wait for progress in computer codes which include lattice dynamics.

Finally, we can combine our value for ^{44}Sc in TiO_2 (rutile) of $\nu_Q=eQV_{zz}/h=10.27(4)$ MHz with that of ^{45}Sc in TiO_2 (rutile) $\nu_Q=11.02(1)$ MHz (Ref. 5) to derive the ratio of quadrupole moments $Q(^{44}\mathrm{Sc}, I=1)/Q(^{45}\mathrm{Sc}, I=7/2)=0.908(5)$. With $Q(^{45}\mathrm{Sc}, I=7/2)=-0.236(2)$ b (Ref. 5), we finally get $Q(^{44}\mathrm{Sc}, I=1)=\pm 0.214(3)$ b, which is in good agreement with the literature value of 0.21(2) b,[25] but a factor of 7 more accurate.

ACKNOWLEDGMENTS

It a pleasure to thank Shamik Ghosal for his help in data taking and Steffen Jankuhn for his help with the preparation of the paper. This work was supported by the BMBF under Contract No. 05KK4OL1/4.

*Permanent address: Radiochemistry Laboratory, Variable Energy Cyclotron Centre, Bhabha Atomic Research Centre, Kolkata 700064, India.

†butz@physik.uni-leipzig.de; www.uni-leipzig.de/~nfp/

[1] C. J. Howard, T. M. Sabine, and F. Dickson, Acta Crystallogr. B **47**, 462 (1991).

[2] J. K. Burdett, T. Hughbanks, G. J. Miller, J. W. Richardson, Jr., and J. V. Smith, J. Am. Chem. Soc. **109**, 3639 (1987).

[3] T. Toyoda, H. Kawano, Q. Shen, A. Kotera, and M. Ohmori, Jpn. J. Appl. Phys., Part 1 **39**, 3160 (2000).

[4] A. H. C. Chan, J. F. Porter, J. P. Barford, and C. K. Chan, Water Sci. Technol. **44**, 187 (2001).

[5] K. Sato, S. Takeda, S. Fukuda, T. Minamisono, M. Tanigaki, T. Miyake, Y. Maruyama, K. Matsuta, M. Fukuda, and Y. Nojiri, Z. Naturforsch., A: Phys. Sci. **53**, 549 (1998).

[6] G. Withnell and J. C. Glass, Phys. Rev. B **14**, 5106 (1976).

[7] J. M. Adams and G. L. Catchen, Phys. Rev. B **50**, 1264 (1994).

[8] O. Kanert and H. Kolem, J. Phys. C **21**, 3909 (1988).

[9] T. Butz, S. Saibene, Th. Fraenzke, and M. Weber, Nucl. Instrum. Methods Phys. Res. A **284**, 417 (1989).

[10] T. Butz, Hyperfine Interact. **52**, 189 (1989); **73**, 387 (1992) (erratum).

[11] P. Blaha, K. Schwarz, G. K. H. Madsen, D. Kvasnicka, and J. Luitz, *WIEN2k: An Augmented Plane Wave + Local Orbitals Program for Calculating Crystal Properties* (Technische Universität, Wien, 2001).

[12] Z. Wu and R. E. Cohen, Phys. Rev. B **73**, 235116 (2006).
[13] F. Tran, R. Laskowski, P. Blaha, and K. Schwarz, Phys. Rev. B **75**, 115131 (2007).
[14] J. P. Perdew, K. Burke, and M. Ernzerhof, Phys. Rev. Lett. **77**, 3865 (1996).
[15] M. Body, G. Silly, C. Legein, J.-Y Buzare, F. Calvayrac, and P. Blaha, Chem. Phys. Lett. **424**, 321 (2006).
[16] K. Schwarz, C. Ambrosch-Draxl, and P. Blaha, Phys. Rev. B **42**, 2051 (1990).
[17] L. A. Errico, G. Fabricius, and M. Rentería, Phys. Rev. B **67**, 144104 (2003).
[18] K. Sato, H. Akai, and T. Minamisono, Z. Naturforsch., A: Phys. Sci. **53**, 396 (1998).
[19] F. H. Larsen, I. Farnan, and A. S. Lipton, J. Magn. Reson. **178**, 228 (2006), and references therein.
[20] Th. Wenzel, A. Bartos, K. P. Lieb, M. Uhrmacher, and D. Wiarda, Ann. Phys. **504**, 155 (1992).
[21] L. A. Errico, G. Fabricius, M. Rentería, P. de la Presa, and M. Forker, Phys. Rev. Lett. **89**, 055503 (2002).
[22] P. Blaha, D. J. Singh, P. I. Sorantin, and K. Schwarz, Phys. Rev. B **46**, 1321 (1992).
[23] T. Butz and A. Lerf, Phys. Lett. **97A**, 217 (1983).
[24] C. Gabathuler, E. E. Hundt, and E. Brun, in *Magnetic Resonance and Related Phenomena*, edited by V. Hovi (North Holland, Amsterdam, 1973), p. 499.
[25] H. Haas and D. A. Shirley, J. Chem. Phys. **58**, 3339 (1973).